


Multi-Subject Unsupervised Transfer with Weighted Subspace Alignment for Common Spatial Patterns


Zhining Chen

*Department of Cognitive Science
Department of Mathematics
University of California San Diego
La Jolla, USA
zhc008@ucsd.edu*

 0000-0002-9384-3618


Mahta Mousavi

*Uncertainty, Inverse Modeling
and Machine Learning Group
Technische Universität Berlin
Berlin, Germany
mahta@ucsd.edu*

 0000-0002-0139-7295

Virginia R. de Sa

*Department of Cognitive Science
Halicioğlu Data Science Institute
University of California San Diego
La Jolla, USA
desa@ucsd.edu*

 0000-0002-0989-3576

Abstract—Motor imagery classification is known to be highly user dependent. Subspace alignment has been somewhat successful in allowing for unsupervised transfer from one training user to a new user. In this paper we develop a method to weight contributions from subspace alignment to multiple training users to give improved unsupervised transfer performance on the new test user. Ablation analyses show that both the subspace alignment and weighting are critical for improved performance. We also discuss how weighting uses the labels of the training users to better interpret subspace alignment.

Index Terms—Common spatial patterns (CSP), motor imagery, brain-computer interface (BCI), subspace alignment, electroencephalography (EEG), unsupervised transfer learning

I. INTRODUCTION

Motor imagery (MI) brain-computer interface (BCI) is a popular category of BCI systems in which the user imagines parts of her/his body such as the right or left hand and the BCI attempts to detect which limb was imagined by the user [1], [2]. MI-BCI is trained on the electroencephalography (EEG) signal recorded from each user in a calibration session. First, the supervised method of common spatial patterns (CSP) is trained for feature extraction [3] and secondly, a linear classifier on the selected features is trained to select the imagined class [4]. In practice, often times the calibration session is short to avoid fatigue for the user and training of the CSP filters and the classifier are done for each user separately.

Due to the non-stationarity and variations in temporal and spatial information of the motor imagery signal, the quality of the trained classifier is negatively affected when the number of training trials is limited. This is often the case in practice. One way to overcome this limitation is to use existing motor imagery data from other users to train a classifier for a new user. However, as described below, differences in brain anatomy and in motor imagery performance between users [5],

usually results in poor performance for direct transfer of one user’s MI-BCI to another.

The motor imagery signal is user generated and in EEG-based systems this signal is recorded at the scalp; however, the signal recorded at the scalp depends not only on the location of the involved neurons but also the orientation of the neurons’ dendrites which affects the orientation of the current flow [6]. Therefore, the MI signal across users varies and a classifier trained for one user cannot be readily used for another [7], [8]. Even for the same user, frequent recalibration is often necessary to accommodate possible drifts in the generated motor imagery signal [9], [10]. There are many transfer learning attempts that use existing data to train a classifier for a new user in an unsupervised fashion, i.e., with unlabeled calibration data for the new user [11]. Among these methods, subspace alignment [12] finds a linear mapping to adapt the features from the source domain to the target domain, however, it does not use the available labels from the source domain.

In this work, we propose a novel improvement on subspace alignment that utilizes data from multiple users and weights the subspace-aligned features from the source users by how much in agreement they are in their transfer to the target (new) user. Our method does not use labels from the target user and hence is completely unsupervised with respect to the target user, but is able to leverage multiple training users to assess their applicability when subspace aligned with the target user. We compare our proposed method with a few baseline methods and show its superiority in improving the subspace alignment features on three different motor imagery datasets.

II. DATASETS

We test our method on three different EEG motor imagery datasets. Pre-processing and data analyses were done in MATLAB.

A. Dataset Iva, BCI Competition III

This dataset [13] from BCI competition III [14] contains 2-class (right hand and foot) motor imagery EEG data from 5 subjects. Data were originally recorded from 118 Ag/AgCl

This work was supported by NSF IIS 1219200, IIS 1817226, SMA 1041755, and IIS 1528214, FISP G2171, G3155, NIH 5T32MH020002-18, and UC San Diego Mary Anne Fox dissertation year fellowship

electrodes; however, we selected 68 channels for analysis based on [15]. For each subject, 280 trials were available. The size of the training set and test set differed for each subject. For both classes combined, there were 168, 224, 84, 56, 28 training trials and 112, 56, 196, 224, 252 test trials for subjects s1, s2, s3, s4 and s5, respectively. The preprocessing of this dataset replicated the steps in [15] and [16]. The time interval of 0.5-2.5s after cue were selected for each trial and the signal was bandpass filtered between 8-30Hz with Matlab's `butter` function with order 5, which gives a tenth order Butterworth filter.

B. Dataset IIa, BCI Competition IV

This dataset [17] from BCI competition IV [18] contains 4 motor imagery classes (i.e., left hand, right hand, foot, and tongue) from 9 subjects, and we used two of the classes for analysis (left hand and right hand). Data were recorded with 22 Ag/AgCl electrodes. For each subject, there were 72 training trials and 72 test trials per class. The preprocessing of this dataset was the same as the procedure used for Dataset IVa, BCI competition III. The time interval of 0.5-2.5s after the cue were selected for each trial and the signal was bandpass filtered between 8-30Hz with Matlab's `butter` function with order 5, which gives a tenth order Butterworth filter.

C. Dataset Three

This dataset from [10], [19] contains 2-class (left hand and right hand) motor imagery EEG data from 12 subjects. Data were recorded with 64 channels. After balancing the right and left trials, for each subject, there were 93 one-second trials per class in the training session. In the test session, there were 179, 215, 85, 238, 169, 282, 211, 208, 181, 269, 111, 248 trials per class for subjects s1 to s12 respectively. The preprocessing of this dataset used the code from [19]. Data were filtered between 7-30 Hz Matlab's `butter` function with order 3, which gives a sixth order Butterworth filter.

III. METHODS

A. Common Spatial Patterns (CSP)

Motor imagery results in desynchronization (or decreased power) of EEG activity in alpha/mu (8-13 Hz) and beta (13-30 Hz) frequency bands over the relevant areas of somato-motor cortex. For distinguishing between motor imagery of two different body parts, it is critical to discriminate spatial differences in this desynchronization at the scalp. Common spatial patterns (CSP) is one of the most commonly used algorithms for extracting such features. CSP finds spatial filters that maximize the variance (or power) of the band-limited spatially filtered signals from one class while minimizing it for the other class [3], [4]. Let ξ_i be the i th trial from a preprocessed EEG dataset, and $\xi_i \in \mathbb{R}^{C \times T}$, where C is the number of EEG channels and T is the number of time samples. For each of the two classes, N_1 and N_2 represent

the set comprising trials for classes 1 and 2, respectively. The normalized covariance matrix Σ_y can be estimated as:

$$\Sigma_y = \frac{1}{|N_y|} \sum_{i \in N_y} \frac{\xi_i \xi_i^\top}{\text{trace}(\xi_i \xi_i^\top)} \quad (1)$$

where $y \in \{1, 2\}$ and $|N_y|$ represents the number of trials in N_y , ξ_i^\top indicates the transpose of ξ_i , and the trace is the sum of the diagonal entries. The CSP filter that maximizes variance for class 1 (while minimizing it for class 2) can be found by maximizing the following objective function:

$$\max_w \frac{w^\top \Sigma_1 w}{w^\top (\Sigma_1 + \Sigma_2) w}. \quad (2)$$

A full set of filters can be optimized by solving the generalized eigenvalue problem $\Sigma_1 w = \lambda(\Sigma_1 + \Sigma_2)w$ [4]. Concatenating the eigenvectors corresponding to the m largest and smallest eigenvalues as columns of matrix W , the spatially filtered signal of a trial ξ_i is obtained as $Z = W^\top \xi_i$. The feature extracted by the k th spatial filter is:

$$f_k = \log \left(\frac{\text{var}(Z_k)}{\sum_{j=1}^{2m} \text{var}(Z_j)} \right) \quad (3)$$

where Z_k ($k = 1 \dots 2m$) is the k th row of matrix Z . In this paper, we used $m = 3$ for the CSP parts of all algorithms as is commonly used [4].

B. Subspace Alignment (SA)

Subspace alignment (SA) is an algorithm proposed by Fernando *et al.* [12], and it is has been widely used for domain adaptation [20] [21]. We used this algorithm to reduce the domain discrepancy between training and test data in our method. In SA, given source data X_S and target data X_T , principal component analysis (PCA) is applied separately to the training and test data to produce a lower dimensional source subspace S_S and lower dimensional target subspace S_T . Then X_S and X_T are each projected to their respective subspaces by $X_S S_S$ and $X_T S_T$. The source subspace is then mapped to the target subspace through linear transformation. The transformation matrix M is learned by minimizing the Bregman matrix divergence:

$$M^* = \underset{M}{\text{argmin}} (||S_S M - S_T||_F^2) \quad (4)$$

where $|| \cdot ||_F^2$ is the Frobenius norm. The Frobenius norm has the orthogonal invariance property, so Equation (4) can be rewritten as:

$$\begin{aligned} M^* &= \underset{M}{\text{argmin}} (||S_S^\top S_S M - S_S^\top S_T||_F^2) \\ &= \underset{M}{\text{argmin}} (||M - S_S^\top S_T||_F^2). \end{aligned} \quad (5)$$

The solution to the above is $M^* = S_S^\top S_T$, and thus the subspace aligned coordinate system is $S_a = S_S S_S^\top S_T$. The subspace alignment [12] algorithm is presented in Algorithm 1. We used 2 dimensional subspaces on Dataset IVa from BCI competition III and Dataset IIa from BCI competition IV. For

Dataset Three, we determined the dimension by using subject 1’s training data as training and subject 12’s training data as test data and vice versa. We performed CSP with SA with different dimensions and looked at the classification accuracy of LDA on subject 1 and 12’s training data. The dimension determined for Dataset Three was 6. No test data for any subject was used in this selection process.

Algorithm 1: Subspace Alignment [12]

Input: Source data X_S , Target data X_T , Subspace dimension d

Output: Subspace aligned data X_{S_a}, X_{T_a}

$S_S \leftarrow PCA(S, d);$

$S_T \leftarrow PCA(T, d);$

$S_a \leftarrow S_S S_S^\top S_T;$

$X_{S_a} = S_S S_a;$

$X_{T_a} = S_T S_a;$

return X_{S_a}, X_{T_a}

C. Proposed Algorithm: SA_weighted

Let $\{X_1 \dots X_n\}$ indicate EEG data from n subjects where subject j is the selected test subject and the rest are training subjects. Each subject contains training trials X^{tr} and test trials X^{te} , and trials are labeled with -1 (class 1) and 1 (class 2).

This algorithm loops through each of the training subjects. For a training subject i , CSP is trained from labeled training trials X_i^{tr} . Then CSP filters are applied to subject i ’s training trials X_i^{tr} and the test subject’s test trial X_j^{te} to extract corresponding features. Subspace alignment is then applied to the extracted features to perform domain adaptation. Then Linear Discriminant Analysis (LDA) is trained on the aligned training features and produces a prediction of the labels of the aligned test features. The prediction is produced based on subject i ’s training data, so it is named $prediction_i$.

After getting $prediction_i$, an inner loop is used to determine the weighting for $prediction_i$. The inner loop loops through subjects other than i and our test subject j . For a subject k in the inner loop, the features of his/her training data X_k^{tr} are extracted by the CSP filters trained on X_i^{tr} from the outer loop. Subspace alignment is then applied to the extracted features of X_k^{tr} and X_j^{te} . LDA is trained on the aligned training features from subject k and produces a prediction of the labels of the aligned test features. This prediction is trained on subject k ’s training data, so it is named $prediction_k$.

For each test trial of the test subject, the inner loop predictions from every training subject k are added together. Since the labels of the predictions are either -1 or 1, then after addition, the *sign* function is applied to get the combined predicted labels. $prediction_i$ is then compared with the combined predicted labels to see $prediction_i$ ’s agreement rate with the combined labels. The agreement rate is compared with 0.5

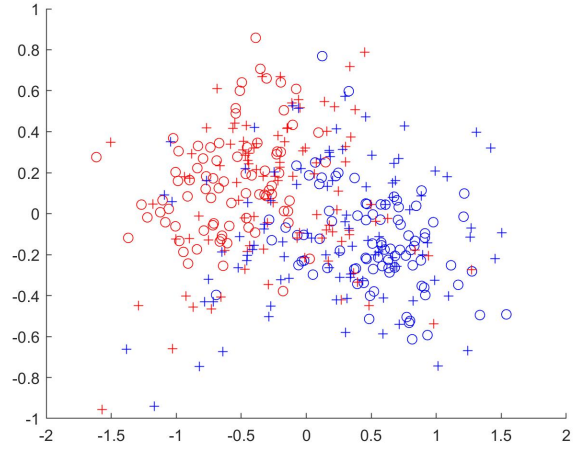


Fig. 1. Subspace alignment results of subject 1 and subject 3 from dataset IVa BCI competition III. The training data of subject 1 (circles) and test data of subject 3 (crosses) are aligned. The color represents the label of the trials, where red represents class 1 and blue represents class 2.

before being used as the weighting for $prediction_i$ to generate an ensemble prediction in the outer loop through:

$$ensemble_prediction = \sum_{i=1}^n weight_i * prediction_i \quad (6)$$

An agreement rate below chance level would suggest that this subject has opposite prediction compared to others, and it is possible that the subspace alignment has mapped class one training data closer to class two test data. We will explain this with an example:

In Fig. 1 and Fig. 2, we plotted the features of subject 1’s training data and subject 3’s test data after SA from dataset IVa, BCI competition III. Fig. 1 shows the results with the correct labels for subject 1 and subject 3. But, SA is unsupervised, so if we switch the labels of training data from class one and class two for subject 1, the SA results don’t change (Fig. 2). SA generally works due to a tendency for subjects to be somewhat aligned (for example due to contralateral cortical organization for right vs left imagery), but as it is unsupervised, misalignment is still possible, and if they are close to 180 degrees out of phase, the alignment can still be very useful if the signs are flipped.

The final predicted labels of the test data X_j^{te} are generated after applying the *sign* function to the *ensemble_prediction*. The pseudo-code for SA_weighted is depicted in Algorithm 2.

D. Baseline Algorithms

We included the results of the supervised CSP algorithm (called *CSP*) with LDA for classification, as a reference for the performance of the unsupervised algorithms.

The unweighted version of our proposed algorithm (called *unweighted*) and the weighted but without SA version (called

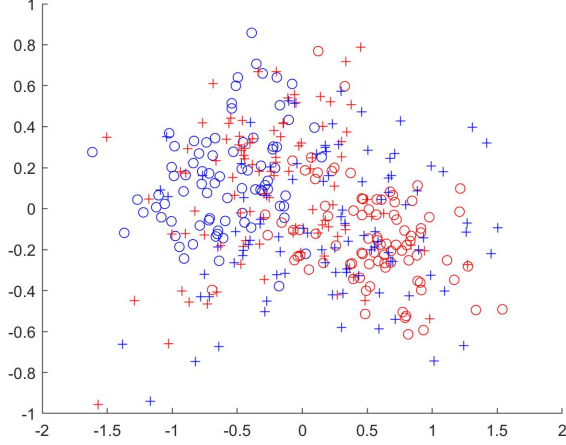


Fig. 2. Subspace alignment results of subject 1 and subject 3 from dataset IVa BCI competition III after manually reversing the labels of subject 1's data before SA. The training data of subject 1 (circles) and test data of subject 3 (crosses) are aligned. The color represents the label of the trials, where red represents class 1 and blue represents class 2.

Algorithm 2: The proposed algorithm: SA_weighted

Input: n subjects' training data $\{X_1^{tr} \dots X_n^{tr}\}$ and the j th subjects' test data X_j^{te}
Output: prediction of X_j^{te} 's labels
initialize *ensemble_pred* as a zero array;
for $i = 1 : n$ and $i \neq j$ **do**
 load training data $X_{i_1}^{tr}$ for class 1 and $X_{i_2}^{tr}$ for class 2;
 initialize Σ_{i_1} and Σ_{i_2} as the average covariance matrix of $X_{i_1}^{tr}$ and $X_{i_2}^{tr}$;
 $W_i = CSP(\Sigma_{i_1}, \Sigma_{i_2})$;
 calculate features f_i^{tr} and f_j^{te} using W_i ;
 construct aligned subspace $X_{sa_i}^{tr}$ and $X_{sa_j}^{te}$;
 train LDA using $X_{sa_i}^{tr}$;
 apply LDA on $X_{sa_j}^{te}$ to get *prediction_i*;
 initialize *pseudoLabel_i* as an zero array;
 for $k = 1 : n$ and $k \neq j$ and $k \neq i$ **do**
 calculate features f_k^{tr} and f_j^{te} using W_i ;
 construct aligned subspace $X_{sa_k}^{tr}$ and $X_{sa_j}^{te}$;
 train LDA using $X_{sa_k}^{tr}$;
 apply LDA on $X_{sa_j}^{te}$ to get *prediction_k*;
 pseudoLabel_i += *prediction_k*;
 end
 pseudoLabel_i = *sign(pseudoLabel_i)*;
 weight = $0.5 - ((\text{sum}(|\text{pseudoLabel}_i - \text{prediction}_i|) / \text{number of trials}) / 2)$;
 ensemble_pred += *weight* * *prediction_i*;
end
labels = *sign(ensemble_pred)*;
return *labels*

noSA) are ablation analyses included separately for compari-

son to the full algorithm, i.e., *SA_weighted*.

We also include another method (called *combine*) which involves concatenating the training data from all training subjects and learning one set of CSP filters and LDA classifier for all the training data. The CSP filters and LDA classifier is then applied to the test data from the test subject. This method serves as a baseline for unsupervised transfer learning.

The *combine_SA* is another baseline algorithm that we used to compare the results with our proposed algorithm. *combine_SA* is identical to the *combine* algorithm except that SA is applied to the test data to align it with the combined training data. The pseudo-code for this algorithm is depicted in Algorithm 3.

Algorithm 3: Combine_SA

Input: n training dataset $\{X_n^{tr} \dots X_n^{tr}\}$ and the j th test dataset X_j^{te}
Output: prediction of X_j^{te} 's label
initialize $X_{combine_1}^{tr}$ and $X_{combine_2}^{tr}$ as empty cells;
for $i = 1 : n$ and $i \neq j$ **do**
 load training data $X_{i_1}^{tr}$ for class 1 and $X_{i_2}^{tr}$ for class 2;
 append $X_{i_1}^{tr}$ into $X_{combine_1}^{tr}$ and append $X_{i_2}^{tr}$ into $X_{combine_2}^{tr}$;
end
initialize Σ_1, Σ_2 as the average covariance matrix of $X_{combine_1}^{tr}$ and $X_{combine_2}^{tr}$;
 $W = CSP(\Sigma_1, \Sigma_2)$;
calculate features f^{tr} and f_j^{te} using W ;
construct aligned subspace X_{sa}^{tr} and X_{sa}^{te} ;
train LDA using X_{sa}^{tr} ;
apply LDA on X_{sa}^{te} to get *prediction*;
return *prediction*

IV. RESULTS

We tested the prediction accuracy of different methods on the three datasets. The accuracy results on dataset IVa from BCI competition III, dataset IIa from BCI competition IV, and dataset Three are presented in Table I, Table II, and Table III respectively. In Table I and Table II, the proposed *SA_weighted* algorithm outperforms the other unsupervised methods, while it is close to *combine_SA* in Table II. In Table III, *combine_SA* outperforms the rest of the algorithms, but the accuracy of *SA_weighted* is comparable or better among all methods.

The weightings found by our algorithm are shown in Fig. 3, Fig. 4 and Fig. 5. While generally positive, there are some notable negative values which, as mentioned earlier, are possibly due to SA being an unsupervised algorithm.

V. DISCUSSION

We have presented a method for unsupervised transfer by weighting predictions from different training subjects after subspace alignment to the test subject. This method performs generally well across different datasets and in several cases

TABLE I
RESULTS OF METHODS ON DATASET IVA FROM BCI COMPETITION III.

subjects	supervised CSP	unsupervised				
		unweighted	noSA	SA_weighted	combine	combine_SA
s1	0.7321	0.7143	0.4554	0.7589	0.6875	0.3661
s2	0.9821	0.8214	0.4821	0.7679	0.4821	0.3571
s3	0.6378	0.5663	0.5204	0.6378	0.5306	0.5510
s4	0.8884	0.4955	0.4911	0.7634	0.5357	0.6830
s5	0.7698	0.7222	0.5000	0.7341	0.6468	0.7381
Mean	0.8021	0.6640	0.4898	0.7324	0.5766	0.5391

TABLE II
RESULTS OF METHODS ON DATASET IIA FROM BCI COMPETITION IV.

subjects	supervised CSP	unsupervised				
		unweighted	noSA	SA_weighted	combine	combine_SA
s1	0.9028	0.8264	0.7639	0.8542	0.8611	0.8403
s2	0.5833	0.5833	0.5347	0.6111	0.6250	0.6111
s3	0.9722	0.9097	0.9306	0.9306	0.9444	0.9444
s4	0.6875	0.6806	0.5139	0.6806	0.5208	0.6319
s5	0.5000	0.5764	0.5903	0.5694	0.5278	0.5833
s6	0.6806	0.5347	0.5139	0.6111	0.5347	0.6250
s7	0.8056	0.5556	0.5972	0.6806	0.6736	0.7153
s8	0.9444	0.9236	0.8958	0.9514	0.9722	0.9653
s9	0.9236	0.7222	0.5903	0.7569	0.6319	0.6250
Mean	0.7778	0.7014	0.6590	0.7384	0.6991	0.7269

TABLE III
RESULTS OF METHODS ON DATASET THREE. THE * BESIDES s1 AND s12 INDICATE THAT THEIR TRAINING DATA WERE USED TO DETERMINE THE DIMENSION OF SA. NOTE THAT THE TEST DATA OF THESE SUBJECTS WERE NOT USED FOR THIS PURPOSE.

subjects	supervised CSP	unsupervised				
		unweighted	noSA	SA_weighted	combine	combine_SA
s1*	0.6237	0.7293	0.6366	0.7087	0.7944	0.7966
s2	0.5377	0.6109	0.5769	0.6212	0.6784	0.6753
s3	0.7447	0.6535	0.5824	0.6435	0.6471	0.7206
s4	0.7120	0.6218	0.5126	0.6233	0.6408	0.6739
s5	0.6334	0.7148	0.6138	0.7472	0.6438	0.6876
s6	0.5156	0.5489	0.5059	0.5472	0.5246	0.5748
s7	0.6642	0.5806	0.5235	0.6085	0.5154	0.5863
s8	0.6221	0.5808	0.5786	0.5873	0.5938	0.5856
s9	0.7229	0.6088	0.5033	0.6304	0.6956	0.7127
s10	0.5041	0.6158	0.5385	0.6067	0.5857	0.5980
s11	0.6932	0.6113	0.5581	0.5966	0.5482	0.5640
s12*	0.4873	0.5014	0.5018	0.4980	0.4694	0.4677
Mean	0.6218	0.6148	0.5526	0.6182	0.6114	0.6369

outperforms the supervised performance obtained by training only on each subject's own training data. Dataset IVa from BCI competition III has different numbers of training trials for each subject, and our method outperforms other unsupervised transfer algorithms presented in Table 1. The bias caused by different training set sizes has a strong influence on methods like *combine_SA* while it inflicts little influence on our method as we are weighting the predicted labels created by each training model based on their agreement with other subjects.

For Dataset IIA from BCI competition IV and Dataset Three, each subject has the same number of training trials, and our method performs comparably to others. In Dataset Three, *combine_SA* outperforms our method, and we found that the weightings for each training subject in Dataset Three have less variability (except for s6, s10, and s12, which have poor performance on supervised CSP) compared to those in the

other two datasets. The less variability in weightings causes the method to perform more like the unweighted version. Even though it does not improve the overall accuracy, the lower weightings on the less reliable training subjects is a valuable feature and improves performance on some subjects.

REFERENCES

- [1] Luis Fernando Nicolas-Alonso and Jaime Gomez-Gil. Brain computer interfaces, a review. *Sensors*, 12(2):1211–1279, 2012.
- [2] Gert Pfurtscheller, Clemens Brunner, Alois Schlögl, and FH Lopes Da Silva. Mu rhythm (de) synchronization and EEG single-trial classification of different motor imagery tasks. *NeuroImage*, 31(1):153–159, 2006.
- [3] Herbert Ramoser, Johannes Muller-Gerking, and Gert Pfurtscheller. Optimal spatial filtering of single trial EEG during imagined hand movement. *IEEE Transactions on Rehabilitation Engineering*, 8(4):441–446, 2000.

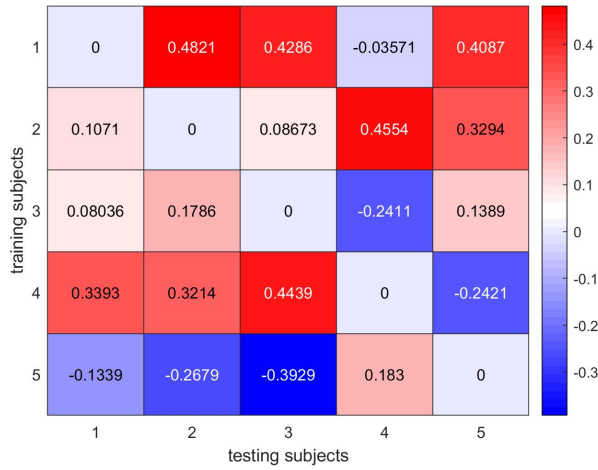


Fig. 3. Weightings in $SA_weighted$ on Dataset IVa from BCI competition III

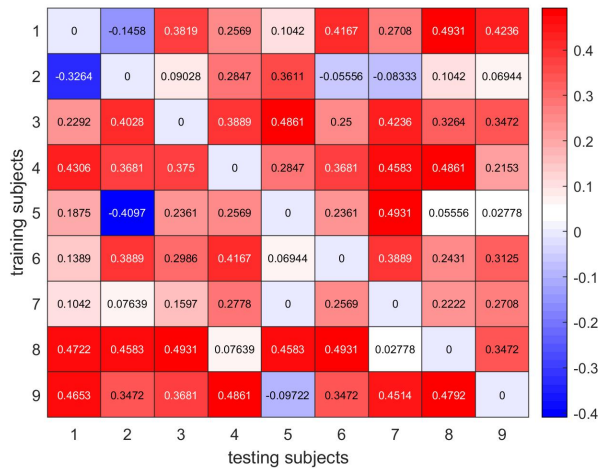


Fig. 4. Weightings in $SA_weighted$ on Dataset IIa from BCI competition IV

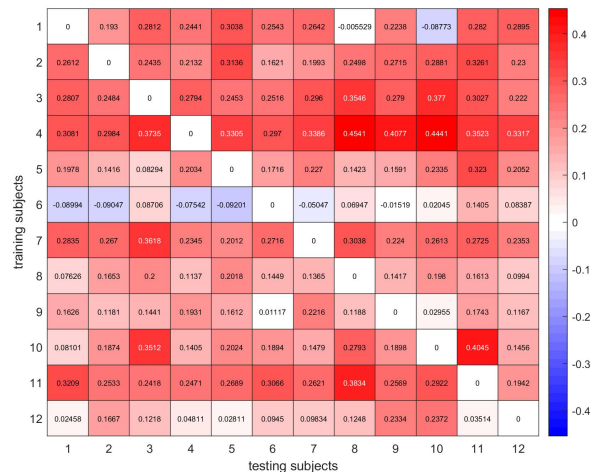


Fig. 5. Weightings in $SA_weighted$ on Dataset Three

[4] Benjamin Blankertz, Ryota Tomioka, Steven Lemm, Motoaki Kawanabe, and K-R Muller. Optimizing spatial filters for robust EEG single-trial analysis. *IEEE Signal Processing Magazine*, 25(1):41–56, 2008.

[5] Mahta Mousavi and Virginia R de Sa. Towards elaborated feedback for training motor imagery brain computer interfaces. In *Proceedings of the 7th Graz Brain-Computer Interface Conference 2017*, pages 332–337, 2017.

[6] Hans Hallez, Bart Vanrumste, Roberta Grech, Joseph Muscat, Wim De Clercq, Anneleen Vergult, Yves D’Asseler, Kenneth P Camilleri, Simon G Fabri, Sabine Van Huffel, and Ignace Lemahieu. Review on solving the forward problem in EEG source analysis. *Journal of Neuroengineering and Rehabilitation*, 4:46, 2007.

[7] Fabien Lotte, Laurent Bougrain, Andrzej Cichocki, Maureen Clerc, Marco Congedo, Alain Rakotomamonjy, and Florian Yger. A review of classification algorithms for EEG-based brain–computer interfaces: a 10 year update. *Journal of Neural Engineering*, 15(3):031005, 2018.

[8] Yiming Jin, Mahta Mousavi, and Virginia R de Sa. Adaptive CSP with subspace alignment for subject-to-subject transfer in motor imagery brain-computer interfaces. In *2018 6th International Conference on Brain-Computer Interface (BCI)*, pages 1–4. IEEE, 2018.

[9] Pradeep Shenoy, Matthias Krauledat, Benjamin Blankertz, Rajesh PN Rao, and Klaus-Robert Müller. Towards adaptive classification for BCI. *Journal of Neural Engineering*, 3(1):R13, 2006.

[10] Mahta Mousavi and Virginia R de Sa. Motor imagery performance from calibration to online control in EEG-based brain-computer interfaces. In *2021 10th International IEEE/EMBS Conference on Neural Engineering (NER)*, pages 491–494. IEEE, 2021.

[11] Zitong Wan, Rui Yang, Mengjie Huang, Nianyin Zeng, and Xiaohui Liu. A review on transfer learning in EEG signal analysis. *Neurocomputing*, 421:1–14, 2021.

[12] Basura Fernando, Amaury Habrard, Marc Sebban, and Tinne Tuytelaars. Subspace alignment for domain adaptation. *arXiv preprint arXiv:1409.5241*, 2014.

[13] Benjamin Blankertz, K-R Muller, Dean J Krusienski, Gerwin Schalk, Jonathan R Wolpaw, Alois Schlogl, Gert Pfurtscheller, Jd R Millan, Michael Schroder, and Niels Birbaumer. The BCI competition III: Validating alternative approaches to actual BCI problems. *IEEE Transactions on Neural Systems and Rehabilitation Engineering*, 14(2):153–159, 2006.

[14] Guido Dornhege, Benjamin Blankertz, Gabriel Curio, and K-R Muller. Boosting bit rates in noninvasive EEG single-trial classifications by feature combination and multiclass paradigms. *IEEE Transactions on Biomedical Engineering*, 51(6):993–1002, 2004.

[15] Wojciech Samek, Carmen Vidaurre, Klaus-Robert Müller, and Motoaki Kawanabe. Stationary common spatial patterns for brain–computer interfacing. *Journal of Neural Engineering*, 9(2):026013, 2012.

[16] Fabien Lotte and Cuntai Guan. Regularizing common spatial patterns to improve BCI designs: unified theory and new algorithms. *IEEE Transactions on Biomedical Engineering*, 58(2):355–362, 2011.

[17] Muhammad Naeem, Clemens Brunner, Robert Leeb, Bernhard Graimann, and Gert Pfurtscheller. Separability of four-class motor imagery data using independent components analysis. *Journal of Neural Engineering*, 3(3):208, 2006.

[18] Michael Tangermann, Klaus-Robert Müller, Ad Aertsen, Niels Birbaumer, Christoph Braun, Clemens Brunner, Robert Leeb, Carsten Mehring, Kai J Miller, Gernot Mueller-Putz, et al. Review of the BCI competition IV. *Frontiers in Neuroscience*, 6:55, 2012.

[19] Mahta Mousavi, Laurens Ruben Krol, and Virginia de Sa. Hybrid brain-computer interface with motor imagery and error-related brain activity. *Journal of Neural Engineering*, 2020.

[20] Shuai Di, Honggang Zhang, Chun-Guang Li, Xue Mei, Danil Prokhorov, and Haibin Ling. Cross-domain traffic scene understanding: A dense correspondence-based transfer learning approach. *IEEE Transactions on Intelligent Transportation Systems*, 19(3):745–757, 2018.

[21] Rong Gui, Xin Xu, Rui Yang, Lei Wang, and Fangling Pu. Statistical scattering component-based subspace alignment for unsupervised cross-domain polar image classification. *IEEE Transactions on Geoscience and Remote Sensing*, 59(7):5449–5463, 2021.